



Summer atmospheric boundary layer structure in the hinterland of Taklimakan Desert, China

WANG Minzhong^{1,2*}, WEI Wenshou^{1,2}, HE Qing^{1,2}, YANG Yuhui³, FAN Lei^{1,2}, ZHANG Jiantao^{1,2}

¹ Institute of Desert Meteorology, China Meteorological Administration, Urumqi 830002, China;

² Taklimakan Desert Atmospheric Environment Observation Experimental Station, Tazhong 841000, China;

³ School of Geographic Science and Tourism, Xinjiang Normal University, Urumqi 830054, China

Abstract: Understanding the characteristics of the structure of desert atmospheric boundary layer and its land surface process is of great importance to the simulations of regional weather and climate. To investigate the atmospheric boundary layer structure and its forming mechanism of Taklimakan Desert, and to improve the accuracy and precision of regional weather and climate simulations, we carried out a GPS radiosonde observation experiment in the hinterland of Taklimakan Desert from 25 June to 3 July, 2015. Utilizing the densely observed sounding data, we analyzed the vertical structures of daytime convective boundary layer and nighttime stable boundary layer in summer over this region, and also discussed the impacts of sand-dust and precipitation events on the desert atmospheric boundary layer structure. In summer, the convective boundary layer in the hinterland of Taklimakan Desert developed profoundly and its maximum height could achieve 4,000 m; the stable boundary layer at nighttime was about 400–800-m thick and the residual mixing layer above it could achieve a thickness over 3,000 m. Sand-dust weather would damage the structures of nighttime stable boundary layer and daytime convective boundary layer, and the dust particle swarm can weak the solar radiation absorbed by the ground surface and further restrain the strong development of convective boundary layer in the daytime. Severe convective precipitation process can change the heat from the ground surface to the atmosphere in a very short time, and similarly can damage the structure of desert atmospheric boundary layer remarkably. Moreover, the height of atmospheric boundary layer was very low when raining. Our study verified the phenomenon that the atmospheric boundary layer with supernormal thickness exists over Taklimakan Desert in summer, which could provide a reference and scientific bases for the regional numerical models to better represent the desert atmospheric boundary layer structure.

Keywords: convective boundary layer; effects of sand-dust and precipitation; GPS radiosonde observation; the hinterland of Taklimakan Desert

Citation: WANG Minzhong, WEI Wenshou, HE Qing, YANG Yuhui, FAN Lei, ZHANG Jiantao. 2016. Summer atmospheric boundary layer structure in the hinterland of Taklimakan Desert, China. *Journal of Arid Land*, 8(6): 846–860. doi: 10.1007/s40333-016-0054-3

The desert atmospheric boundary layer is an important and frontier domain of modern atmospheric science study. Recognizing deeply the characteristics of the structure of desert atmospheric boundary layer and its land surface process is of great importance to the simulations of regional weather and climate, and is helpful for improving the model performance to further increase the accuracy and precision of weather and climate simulations.

*Corresponding author: WANG Minzhong (E-mail: yurenkeji@sina.com)

Received 2015-11-21; revised 2016-04-21; accepted 2016-05-08

© Xinjiang Institute of Ecology and Geography, Chinese Academy of Sciences, Science Press and Springer-Verlag Berlin Heidelberg 2016

In the past decades, domestic and foreign scholars have conducted many studies on the desert atmospheric boundary layer and land surface processes and achieved many significant achievements (Garratt, 1992, 1993; Gamo, 1996; Sivakumar, 2007; Huang et al., 2010). In the 1970s, Charney (1975) studied the albedo and thermal balance of Sahara Desert and the forming mechanism of arid climate, and found that the high surface albedo reduced the net radiation and resulted in the sinking motion in the desert, which reduced the precipitation. Since 1980s, Henderson-Sellers (1980), Gornitz and Nasa (1985), Cunningham and Rowntree (1986) and Lare and Nicholson (1990) conducted detailed analyses on the albedo of different underlying surfaces. Regarding the boundary layer, Marsham et al. (2008) observed a very thick convective boundary layer of 5,500 m with notable residual layer in the Sahara region. Taking advantage of conventional meteorological sounding data, Takemi (1999) analyzed the atmospheric boundary layer structure of Hexi Corridor region of China and conjectured the convective boundary layer with thickness of more than 4,000 m from the characteristics of residual layer. In China, Su and Hu (1987) firstly discovered the “cold-island effect” in the oasis of arid area in the 1980s. Later, Hu and Gao (1994) found the existence of inverse humidity in desert atmosphere adjoining to oasis in the “Heihe River Basin Field Experiment” conducted in the 1990s. To further understand the land-air interactions in typical arid regions, Chinese researchers (Zhang et al., 2007, 2011; Zhang and Wang, 2008) did field observation experiments in the Gobi desert of Dunhuang, Gansu province in 2000. By analyzing the atmospheric boundary layer structure and the land surface process features, they found that a convective boundary layer with the thickness of over 4,000 m exists on clear days in summer in this region. In addition, Wei et al. (2005) studied the wind, temperature and humidity of atmospheric boundary layer in summer over the Jinta oasis of Hexi Corridor, and found that the height of summer boundary layer in this region was about 3,500 m. Using balloon and GPS sounding, Li et al. (2014) investigated the structure of summer atmospheric boundary layer in Badain Jaran Desert and pointed out that the convective mixing layer on clear days in summer could reach up to 3,000 m.

Taklimakan Desert is the second largest mobile desert in the world and extremely sensitive to climate changes in the arid region of Northwest China. The desert has harsh natural environment with extremely dry climate and large scope of mobile sand dunes. Compared with other arid regions in the world, its land surface process and atmospheric boundary layer structure are very unique and have an important influence on the regional weather, climate and atmospheric circulation.

At present, researches on the atmospheric boundary layer of Taklimakan Desert are mainly about the near-surface meteorological observations and analyses (He et al., 2010a, b; Wen et al., 2010; Liu et al., 2012) by using near-surface meteorological observation equipment and remote sensing systems. Although fixed-point continuous observations can be realized, the detection heights and applicable weather conditions are greatly limited, resulting in the restriction of in-depth study of entire atmospheric boundary layer in this desert. He (2009) once studied the land-air interaction and the near-surface thermal structure of desert hinterland deeply and systematically by virtue of an 80-m meteorological tower, and estimated that the convective boundary layer of desert in summer was about 3,000 m. Xu et al. (2014) studied the atmospheric boundary layer structure of Taklimakan Desert using the NCEP (National Centers for Environmental Prediction) reanalysis data, and pointed out that the thickness of convective boundary layer could achieve 3,000–4,000 m. In our previous study (Wang et al., 2012), fiercely developed turbulence was noted on clear days in summer over the desert hinterland, which could reach a height of 3,500–4,000 m. However, the thickness of atmospheric boundary layer needs further verification through radiosonde observation. In this regard, we carried out a GPS radiosonde observation experiment from 25 June to 3 July 2015. Then we used the densely observed sounding data obtained in this experiment to analyze the vertical structures of daytime convective boundary layer and nighttime stable boundary layer, and discussed the effects of sand-dust and precipitation processes on the boundary layer structure. The purposes of this study are to understand more deeply the atmospheric boundary layer structure as well as its developing mechanism over the dry and mobile desert, and also to provide a reference to further study on

boundary layer parameterization in regional numerical models.

1 Study area

Taklimakan Desert is located in the hinterland of Eurasian continent in the mid-latitude of Northern Hemisphere, i.e. in the central part of Tarim Basin in Xinjiang, China. It has Tomur Mountains and Pamir Plateau to its west, Kunlun Mountains and Altun Mountains to its south, Tianshan Mountains to its north and Lop Nur to its east. It is about 1,070 km long from east to west and about 410 km wide from south to north with an area of $33.76 \times 10^4 \text{ km}^2$. It is the second largest mobile desert in the world. In addition, it is a major sand-dust storm source in China. Due to the obstruction effect of Tibetan Plateau and its surrounding mountains, the Taklimakan Desert lies in an extremely arid region with dry winter and few rain in summer. The climate is characterized by sufficient light and heat, few precipitation, strong sunshine and large diurnal temperature difference. Combined with the sparse desert vegetation, a unique and extremely fragile natural ecosystem is formed.

The GPS radiosonde was released at Tazhong ($39^\circ 02' \text{N}$, $83^\circ 38' \text{E}$; Fig. 1), the hinterland of Taklimakan Desert, with an elevation of 1,109 m. The sounding observation field is about 9 km away from the Tazhong Meteorological Station, which is situated in the oil operation area where no sounding balloons are allowed to release. The observation field is an open area with the ground surface covered by mobile sand dunes. Here, the annual mean temperature is 12.1°C , but the highest temperature can reach 46.0°C . The mean annual precipitation is less than 30 mm, but the annual potential evaporation is 3,812.3 mm. East wind prevails in this area with an annual average wind speed of 2.3 m/s. On average, the annual sand-dust storm days are more than 30 d, blowing sand days over 70 d and drifting dust days even beyond 100 d. Such weather often appears through the whole spring and summer. A small amount of desert shrub plants grow in the living quarters of the test field. The underlying surface of the observation field can be representative of Taklimakan Desert.

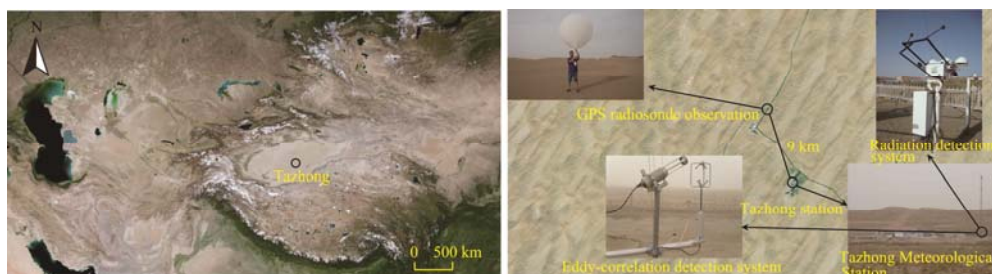


Fig. 1 Sketch map of the study region and observation equipment

2 Data collection and methods

The GPS radiosonde system, radiation observation system and eddy-correlation detection system were used in the experiment (Fig. 1). The GPS sounding system is primarily composed of a surface receiver, an antenna and several sondes. Technical parameters of the GPS sounding system are provided in Table 1. The sounding balloons carried the sondes into sky, and the surface receiver received the radio signal which was transmitted by the sondes and worked out the meteorological information (including atmospheric temperature, humidity, pressure, wind direction and wind velocity). The sounding observation was carried out from 25 June to 3 July 2015, during which the sondes were released six times per day, at 01:15, 07:15, 10:15, 13:15, 16:15 and 19:15 (Beijing time), respectively. The rising speed of sounding balloons was about 300 m/min on average, and the balloons took about 15 min to complete one detecting process of boundary layer. The radiation observation system and eddy-correlation detection system were fixed near the Tazhong Meteorological Station. The radiation observation system was mounted

1.5 m above the ground and equipped with the advanced detecting sensors developed by the Kipp & Zonen Company in the Netherlands. The system could detect the total radiation, reflection radiation, atmospheric long wave radiation and ground long-wave radiation. Net radiation was calculated via the above-mentioned radiation components. All the data were collected at 0.1 Hz and recorded at an interval of 1 min. The eddy-correlation detection system refers to the R3-50 ultrasonic anemometer (Gill Instruments Ltd., UK). It was mounted at a height of 10 m and the data were collected at 20 Hz. The surface sensible heat flux was calculated by the eddy-correlation technique. The surface temperature was observed at the Tazhong Meteorological Station with the soil thermometer. Table 2 presents the major technical parameters of surface observation systems.

Table 1 Technical parameters of GPS sounding system

Type		Manufacturer	Sensor	Measurement range	Detection precision	Error range
GPS sonde	CF-06-A GNSS	Beijing Changfeng Micro-Electronics Technology Co., Ltd., China	Temperature	−90°C–60°C	0.1°C	±0.2°C
			Humidity	0–100%	1%	±3%
			Pressure	3–1,080 hPa	0.1 hPa	±1.0 hPa
			Wind speed	0–150 m/s	0.1 m/s	±0.15 m/s
			Wind direction	0°–360°	0.1°	±2°
Type		Manufacturer	Receiving frequency range	Automatic frequency control precision	Antenna gain	Noise coefficient
Surface receiver	CFL-GNSS-JS	Beijing Changfeng Micro-Electronics Technology Co., Ltd., China	400–406 MHz	2 KHz	>7 dB	2.7 dB

Table 2 Technical parameters of radiation observation system and eddy-correlation detection system

Equipment	Type	Manufacturer	Technical parameter
Short-wave radiometer (total radiation, reflection radiation)	CM21	Kipp & Zonen Company, Netherlands	Spectral range: 305–2,800 nm; sensitivity: 10 $\mu\text{V}/(\text{W}/\text{m}^2)$; response time: getting to 95% in 5 s; direction error: $\leq \pm 10 \text{ W}/\text{m}^2$
Long-wave radiometer (ground long-wave radiation, atmospheric long-wave radiation)	CG4	Kipp & Zonen Company, Netherlands	Spectral range: 4.5–42.0 μm ; sensitivity: 30 $\mu\text{V}/(\text{W}/\text{m}^2)$; warm-up drift: $\leq 4 \text{ W}/\text{m}^2$; response time: getting to 63% in less than 8 s
Ultrasonic anemometer 3-D	R3-50	Gill Instruments Ltd., UK	Sample frequency: 20 Hz; wind speed range: 0–45 m/s; precision: <1% observed wind speed; resolution: 0.01 m/s; wind speed deviation: $< \pm 0.01 \text{ m/s}$; wind direction precision: $\leq \pm 1^\circ$; resolution: 1°

During the observation period, three notable weather processes occurred, i.e. a sand-dust event on 26 June, a short-time sand-dust and rainfall process on 28 June and a severe convective precipitation on 1 July. There was no continuous clear-sky with high temperature during the observation period. Our study mainly focused on analyzing the atmospheric boundary layer structures on 25 June (partly cloudy day), 26 June (sandy and dust day), 29 June (slightly cloudy day) and 1 July (local severe convective precipitation day). According to the requirement of this study, the temperature and relative humidity were converted to the potential temperature and specific humidity, respectively.

Due to the outstanding effect of thermal factors on the process of atmospheric boundary layer in arid desert areas, we used the potential temperature method (Seibert et al., 2000; Hyun et al., 2005; Qiao, 2009) to determine the height of atmospheric boundary layer. The method was to take the inverse potential temperature base of obvious potential temperature jump or fold line as the convective mixing layer height during the daytime observation at 10:15, 13:15, 16:15 and 19:15. That is, the thickness of potential temperature and specific humidity which almost do not change with height is considered as the maximum height of convective mixing layer. During the nighttime (01:15 and 07:15), the near-surface inverse potential temperature top of layer is

considered as the height of stable boundary layer.

3 Results

3.1 Atmospheric boundary layer structure in summer

3.1.1 Vertical distribution of potential temperature

Thermal character is one of the major indicators to judge and distinguish the property of atmospheric boundary layer, and potential temperature is one of the most expressive thermal properties of atmosphere. So, analyzing the vertical distribution of atmospheric potential temperature is of great importance to the recognition of atmospheric boundary layer. Atmospheric boundary layer is generally divided into the daytime convective boundary layer and the nighttime stable boundary layer. The daytime convective boundary layer can be further divided into near-surface layer, convective mixing layer and topped inversion layer (entrainment layer) (Angevine et al., 1994). Figure 2 presents the potential temperature profiles at different layers at six observation times on 25 June 2015 when it was cloudy with high temperature.

As seen from Fig. 2, the potential temperature profiles at 01:15 and 07:15 showed similar structures, and an inversion layer was found near the surface. The thickness of inversion layer was 250 m at 01:15 and developed to 400 m at 07:15, which had the same thickness with the nighttime stable boundary layer. At 01:15, the vertical gradient of potential temperature changed slightly in the heights of 250–3,200 m, which was the remaining mixing layer of last day, also known as the residual mixing layer. There was a residual cover of inversion layer in the heights of 3,200–3,500 m. At 07:15, the heights of residual mixing layer reached up to 400–3,850 m, while the residual cover of inversion layer stayed at the heights of 3,850–4,200 m. Then, free atmosphere was observed above the cover of inversion layer.

It was found that at 10:15 the surface heating destroyed some parts of nighttime stable boundary layer, and a well-mixed layer was formed below 500 m, which was covered by the remaining nighttime stable boundary layer with a depth of 300 m (heights of 500–800 m). The vertical gradient of potential temperature changed slightly at the heights of 800–3,200 m, forming the residual mixing layer. The residual cover of inversion layer lied in the heights of 3,200–3,700 m, which was above the free atmosphere.

At 13:15, the atmosphere was further warmed by surface heating. The convective boundary layer developed to the height of 1,300 m, above which there was a remarkable residual mixing layer and existed a residual cover of inversion layer. Due to the sustained and strong heating effect of ground surface, the convective boundary layer developed abundantly further. At 16:15, the mixing layer reached up to 3,300-m height and at 19:15 it was 4,000 m in height. The mixing layer was covered by a cover of inversion layer with a thickness of about 250 m, i.e. entrainment layer, showing the symbolic feature of upper limit of atmospheric thermal boundary layer. Free atmosphere stayed above the entrainment layer. What needs to be explained is that after the convective mixing layer broke the cover of inversion layer at 16:15, it was mixed with the residual mixing layer in the early stage, driving the convective boundary layer to develop rapidly.

To illustrate the universality of such kind of thick boundary layer features, we provided the potential temperature profiles at 16:15 and 19:15 on 29 June during the observation period (Fig. 3). On 29 June, it was a clear and partly cloudy day, but it rained last evening due to cold air, causing the surface temperature to become lower and further affecting the development of atmospheric boundary layer to some extent on 29 June. The convective boundary layer was about 2,300-m high at 16:15 (Fig. 3a). The vertical gradient of potential temperature changed slightly below 3,000 m at 19:15 (Fig. 3b), indicating that the convective boundary layer may reach the height of 3,000 m or even higher.

The above analysis suggests that over the central part of Taklimakan Desert, the nighttime stable boundary layer is about 400–800 m in thickness, and the residual mixing layer above it has very clear characteristics that it clearly reserves the top covers of daytime mixing layer and inversion layer. During the summer, the thickness of the daytime convective boundary layer is

very large and its maximum height can exceed 4,000 m while the thick residual mixing layer at nighttime can provide very favorable thermal conditions for the development of daytime convective boundary layer. When the daytime convective boundary layer develops and breaks through the inversion layer into the residual layer, the convective boundary layer develops very rapidly and smoothly. The extremely deep convective boundary layer should be attributed to the residual mixing layer in addition to strong surface heating and atmospheric dynamic factors.

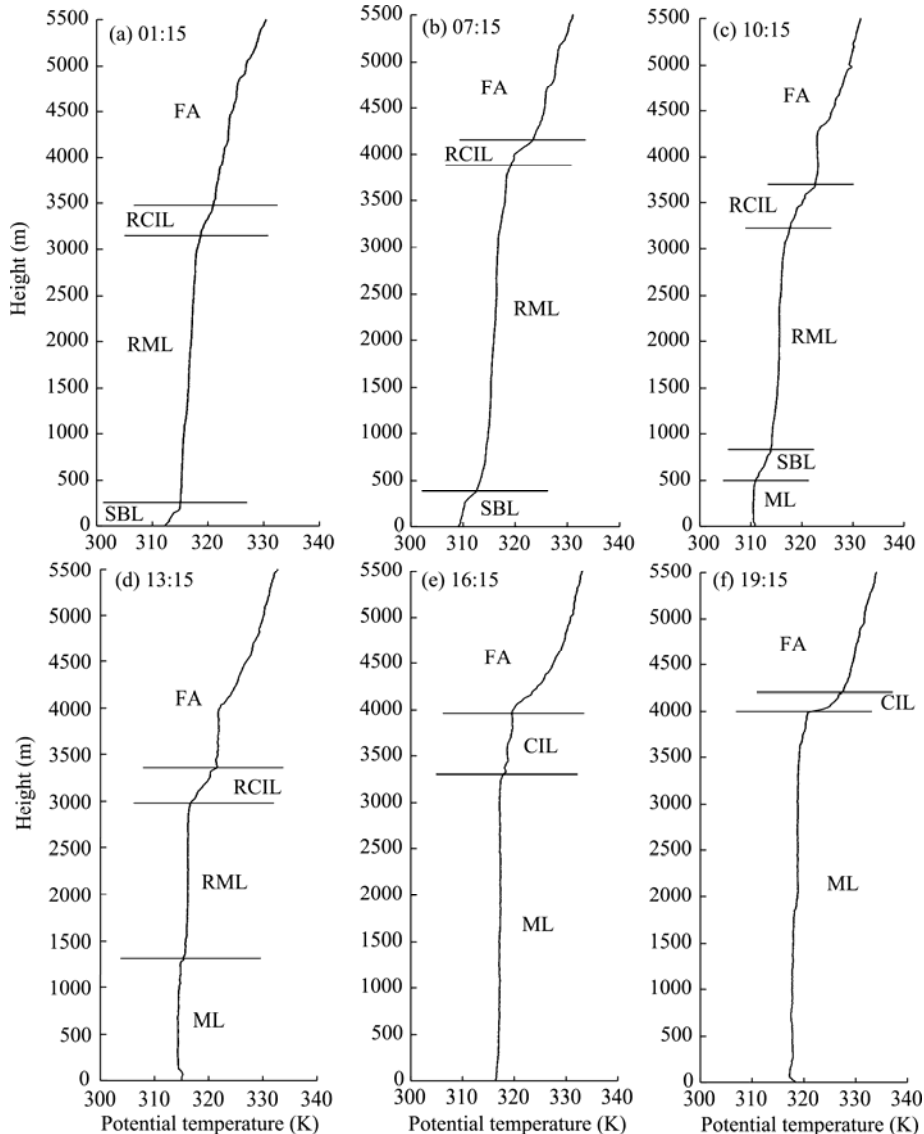


Fig. 2 Potential temperature profiles at different atmospheric heights in the hinterland of Taklimakan Desert at different observation times on 25 June 2015. FA, free atmosphere; ML, mixing layer; RML, residual mixing layer; CIL, cover of inversion layer; RCIL, residual cover of inversion layer; SBL, stable boundary layer.

3.1.2 Vertical distribution of wind speed and specific humidity

Atmospheric boundary layer usually has very obvious dynamic characteristics, greatly influencing the way of atmospheric motion. Generally speaking, the daytime convective boundary layer and the nighttime stable boundary layer show different states of atmosphere. Figure 4 presents the profiles of wind speed at 01:15, 07:15, 10:15, 13:15, 16:15 and 19:15 on 25 June.

The given vertical features of wind speed further illustrate the boundary layer structure

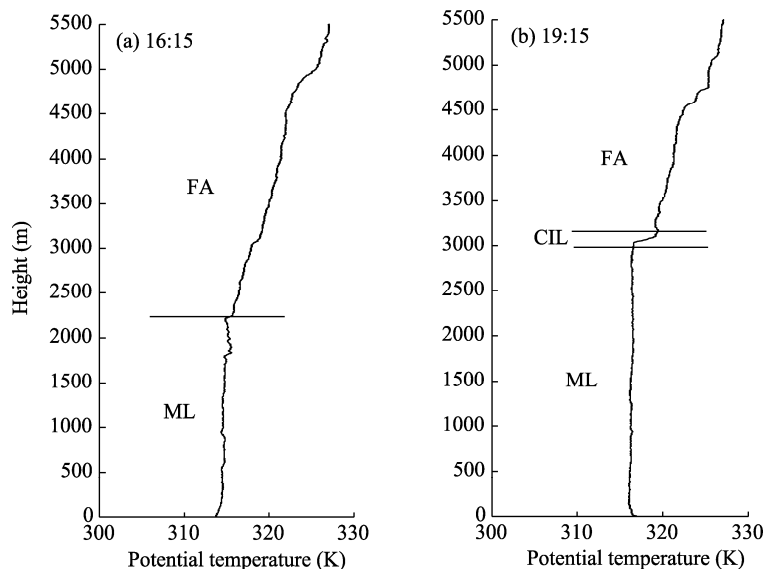


Fig. 3 Potential temperature profiles at different atmospheric heights in the hinterland of Taklimakan Desert at 16:15 (a) and 19:15 (b) on 29 June 2015

is determined by the potential temperature. At nighttime, low-level jet stream was generated on the top of stable boundary layer, and the height of jet was lifted gradually upward along with the rise of stable boundary layer. At 10:15, the jet rose to the height of 800 m or so, corresponding to the height of stable boundary layer. At daytime, the wind speed in the mixing layer increased gradually with increasing height. After getting to the top of convective boundary layer, the wind speed slowed down.

In addition, the thermodynamic and dynamic structures of atmospheric boundary layer affect the distribution of water vapor inside the boundary layer significantly, resulting in the specific humidity distributed differently in the stable boundary layer and convective boundary layer. The profiles of specific humidity on 25 June shown in Fig. 5 revealed that in the nighttime stable boundary layer, the specific humidity (at 01:15 and 07:15) increased upward slightly from the ground surface to the maximum at the top of stable boundary layer. However, in the residual mixing layer, the moisture was well-mixed, indicating that the residual mixing layer affected the distribution of specific humidity. Then, after getting into the top cover of inversion layer which is upon the residual mixing layer, the specific humidity decreased sharply, but further up, the specific humidity began to increase again. In the daytime convective boundary layer, the vertical variation of specific humidity was much smaller, and the profiles of specific humidity maintained a relatively homogeneous state, especially at 16:15 and 19:15, which clearly indicated that the maximum height of daytime convective boundary layer in the hinterland of Taklimakan Desert can reach up to 4,000 m. The specific humidity profiles in Fig. 5 is consistent with the ideal distribution patterns of specific humidity of atmospheric boundary layer provided by other studies (Stull, 1988; Zhang, 2007). Combined with the wind speed profile, we concluded that the reliability of atmospheric boundary layer structure is determined by the potential temperature profile.

Through the comprehensive analyses of potential temperature, wind speed and specific humidity profiles in the hinterland of Taklimakan Desert, we found that the vertical variations of potential temperature, wind speed and specific humidity support one another and verify one another. They can consistently present the typical structure characteristics of summer atmospheric boundary layer in this region.

3.2 Land surface process and its function

Surface thermodynamic factors are closely correlated to the formation, development and dissipation of atmospheric boundary layer. Figures 6a–c show the daily variation curves of land

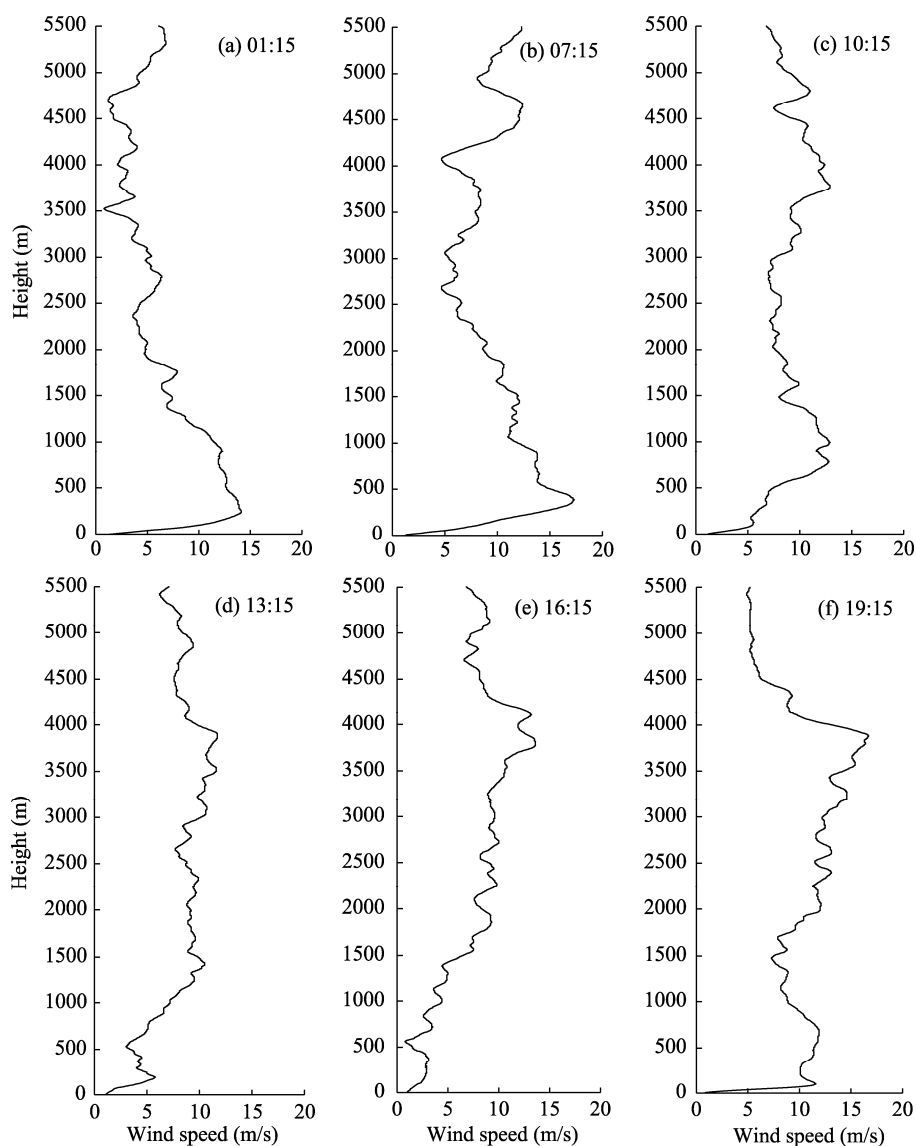


Fig. 4 Wind speed profiles at different atmospheric heights in the hinterland of Taklimakan Desert at different observation times on 25 June 2015

surface net radiation, sensible heat flux and surface temperature in the hinterland of Taklimakan Desert on 25 June 2015. For net radiation, the daily peak value was 280 W/m^2 (Fig. 6a), and for sensible heat flux, the peak value was about 150 W/m^2 (Fig. 6b). Mean annual precipitation in this desert hinterland is less than 30 mm, thus this is an extremely arid area. On hot days in summer, the maximum values of surface net radiation and sensible heat flux can be 400 W/m^2 . However, since it was cloudy on 25 June 2015, the net radiation and sensible heat flux were affected somewhat. The surface temperature rose to 47.4°C during the daytime and dropped to 21.7°C at night (Fig. 6c). The diurnal variation of surface temperature was as large as around 25.7°C , indicating that the ground surface alternately experienced rapidly solar-heated temperature increase and radiation-cooled temperature decrease in Taklimakan Desert. The remarkable increase in temperature caused by the effect of strong surface heating during the daytime provides a powerful external thermodynamic background for exciting the convective activity in the atmospheric boundary layer. Jointly affected by the daytime surface sensible heat flux and the nighttime residual mixing layer, the thick convective boundary layer is prone to form during the daytime over the hinterland of Taklimakan Desert.

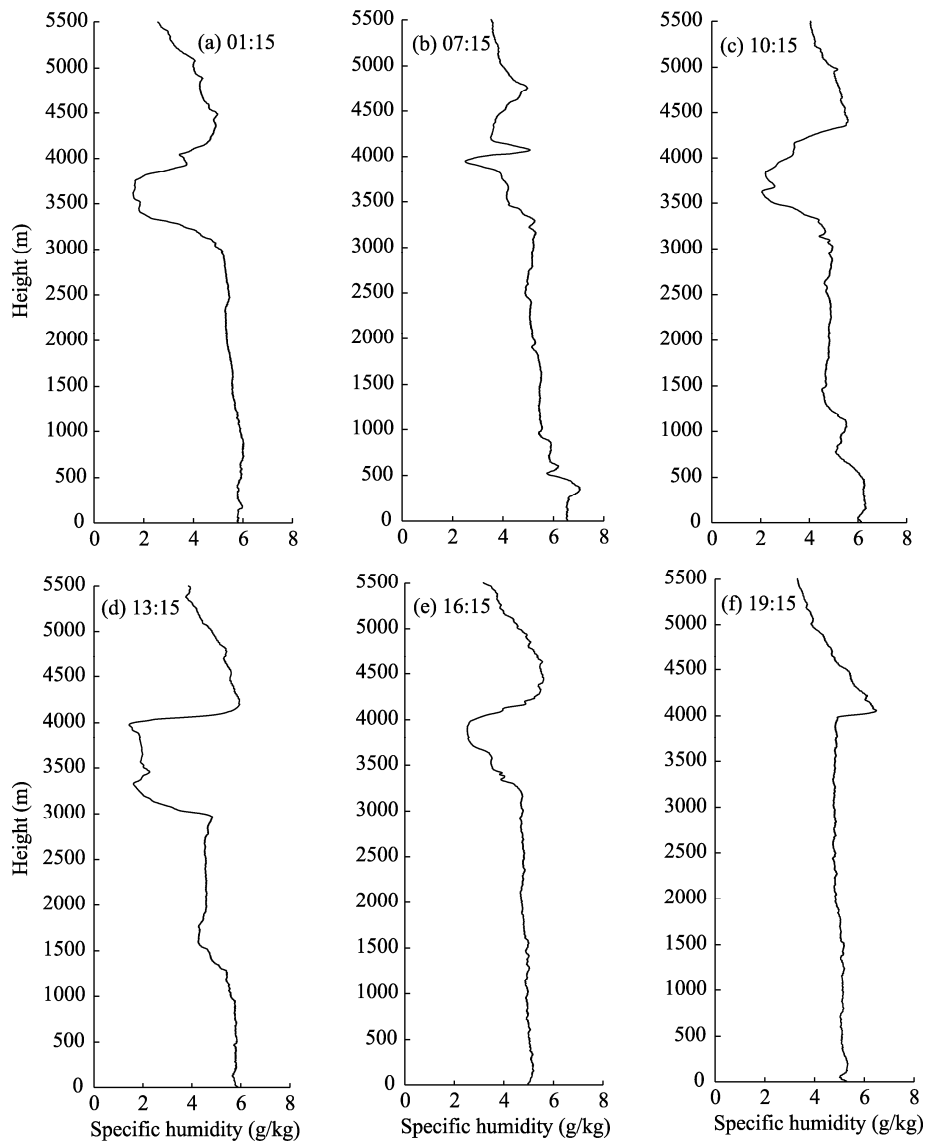


Fig. 5 Specific humidity profiles at different atmospheric heights in the hinterland of Taklimakan Desert at different observation times on 25 June 2015

In this study, we calculated two parameters to further illustrate the characteristics of land surface process and its effect on the development of atmospheric boundary layer. One is the friction velocity (u_*), which represents the turbulent velocity scale, and the other is the convection velocity (w_*), which refers to the convective motion scale. The friction velocity (u_*) can be expressed by Eq. 1 (Deardorff, 1970).

$$u_* = ((\overline{u'w'})^2 + (\overline{v'w'})^2)^{1/4}. \quad (1)$$

Where, u' , v' and w' are transverse pulse wind velocity, longitudinal pulse wind velocity and vertical pulse wind velocity, respectively. They were obtained through the observing of ultrasonic instruments. The convection velocity (w_*) can be expressed as follows (Redelsperger et al., 2000):

$$w_* = \left(\frac{gZ_i}{T_v} (\overline{w'T'_v}) \right)^{1/3}. \quad (2)$$

Where, T_v is the near-surface air virtual potential temperature; Z_i is the thickness of convective

boundary layer; $\overline{w'T'_v}$ is the near-surface sensible heat flux; and g is the gravity acceleration. Parameters T_v , Z_i and $\overline{w'T'_v}$ were determined by the observation data.

Generally, the magnitude of friction velocity is 0.2 m/s, and the convection velocity is about 1.0 m/s (Redelsperger et al., 2000). The friction velocity shows the spreading capability of turbulence to different directions spatially while the convection velocity represents the convective transfer capability in vertical direction. Figures 6d and e are the variation curves of near-surface convection velocity and friction velocity on 25 June 2015 in the hinterland of Taklimakan Desert, respectively. The convection velocity developed from 0.2 to 1.9 m/s at the moment when the heating was the strongest, and the friction velocity was high during the daytime, reaching 0.65 m/s. The results indicated that the convection velocity and friction velocity on this day were both high so that the atmospheric boundary layer can get sufficient convection burst power and favorable dynamic environment condition, which provided a dynamic basis for the convective boundary layer to develop thickly to some extent.

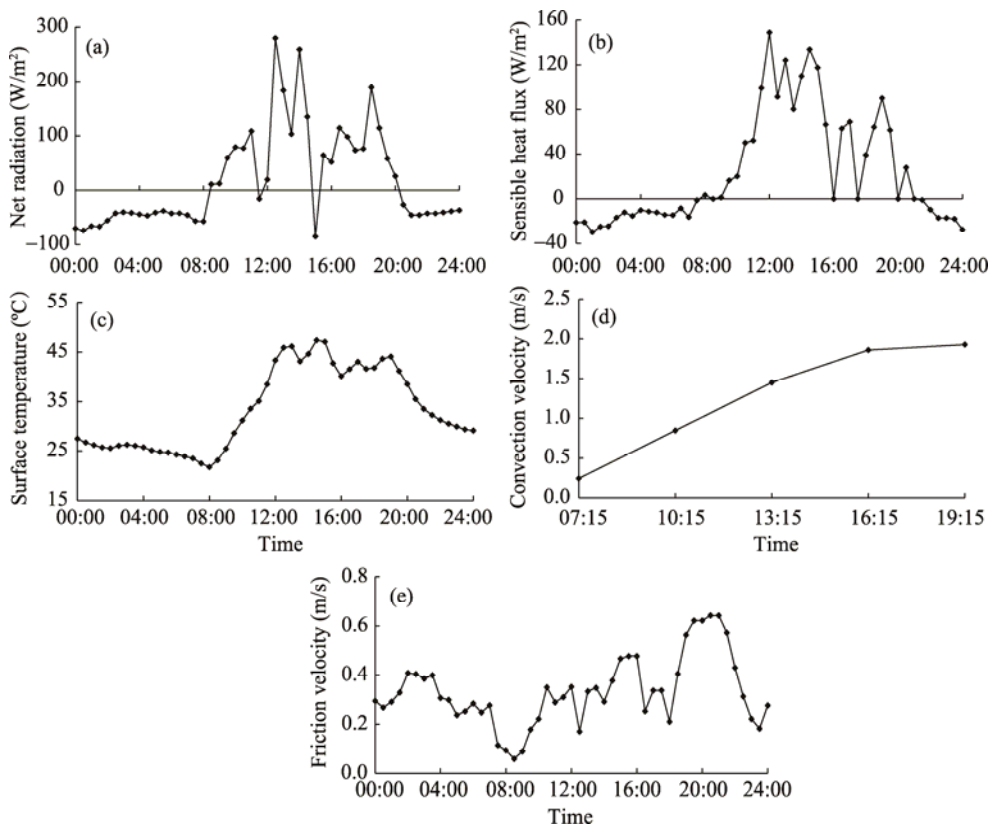


Fig. 6 Daily variations of surface net radiation (a), sensible heat flux (b), surface temperature (c), convection velocity (d) and friction velocity (e) in the hinterland of Taklimakan Desert on 25 June 2015

3.3 Effect of sand-dust weather on atmospheric boundary layer structure

Sand-dust often appears in spring and summer in Taklimakan Desert. During the observation period, one sand-dust event occurred on 26 June 2015. During the period of 00:00–08:00, drifting dust, blowing sand and even sand-dust storm appeared, making the visibility decreased to 761 m only. At daytime, we observed drifting dust during 08:00–14:55 and blowing sand during 14:55–18:03. In order to investigate the structure of atmospheric boundary layer with sand-dust weather, we presented the potential temperature profiles at different atmospheric heights at 01:15, 07:15, 10:15, 13:15 and 19:15 on 26 June (Fig. 7). It should be noted that the GPS sounding system was faulty at 16:15, so no data were collected at the moment.

On 26 June, the potential temperature profile at 01:15 was similar to that at 07:15 (before

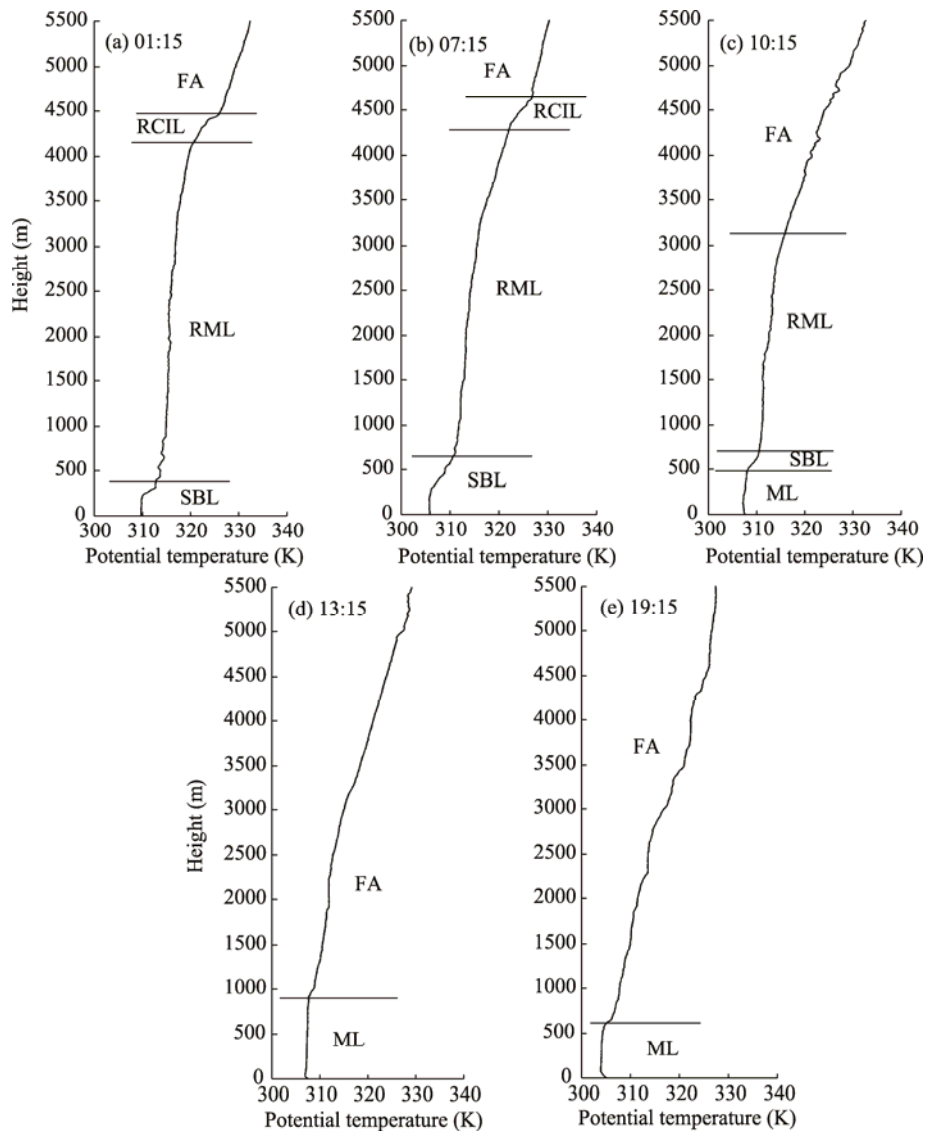


Fig. 7 Potential temperature profiles at different atmospheric heights in the hinterland of Taklimakan desert at different observation times on 26 June 2015

dawn), and the increasing of potential temperature with increasing height was absent from the ground surface to the upper height (Fig. 7). The potential temperature below 250 m remained unchanged, but in the heights of 250–650 m, it increased gradually. Such a phenomenon reveals that the sand-dust event destroyed the nighttime inversion layer to some extent. The sand-dust event weakened the cooling of ground surface at nighttime, and thus no stable boundary layer was clearly formed. However, the residual mixing layer can be clearly distinguished in the heights of 700–4,200 m. The potential temperature profile at 10:15 was similar to that at nighttime, with a 500-m convective boundary layer, above which were the nighttime residual stable boundary layer (500–650 m) and the residual mixing layer (650–3,200 m), and over the two layers was the free atmosphere. At noon 13:15, the convective boundary layer developed to the height of 900 m, but above the height the structure of atmospheric boundary layer became unapparent. During the period of 14:55–18:03, blowing sand event occurred and the situation of atmosphere after the sand-dust event could be clearly shown by the potential temperature profile at 19:15. The result showed that the convective boundary layer dropped to the height of 650 m, above which the potential temperature increased with increasing height, but the structure of boundary layer was

not so clearly seen.

The above analysis suggests that the sand-dust event could damage the structures of nighttime stable boundary layer and daytime convective boundary layer to a certain degree. Due to the occurrence of sand-dust, the dust particle swarm weakens the solar radiation reaching the ground surface, impacts the heat to the atmosphere and depresses the development of daytime convective boundary layer. The maximum thickness of convective boundary layer on 26 June was about 900 m, which was much lower than that on 25 June.

3.4 Impact of precipitation on desert atmospheric boundary layer structure

Taklimakan Desert is located in an extreme arid region with average annual precipitation less than 30 mm. During the observing experimental period, the desert hinterland had an abnormal convective precipitation which lasted for 2 h (16:30–18:30) on 1 July 2015 with the amount of 6.0 mm. Figure 8 exhibited the potential temperature and specific humidity profiles at 13:15, 16:15 and 19:15 (before and after the rainfall) on this day.

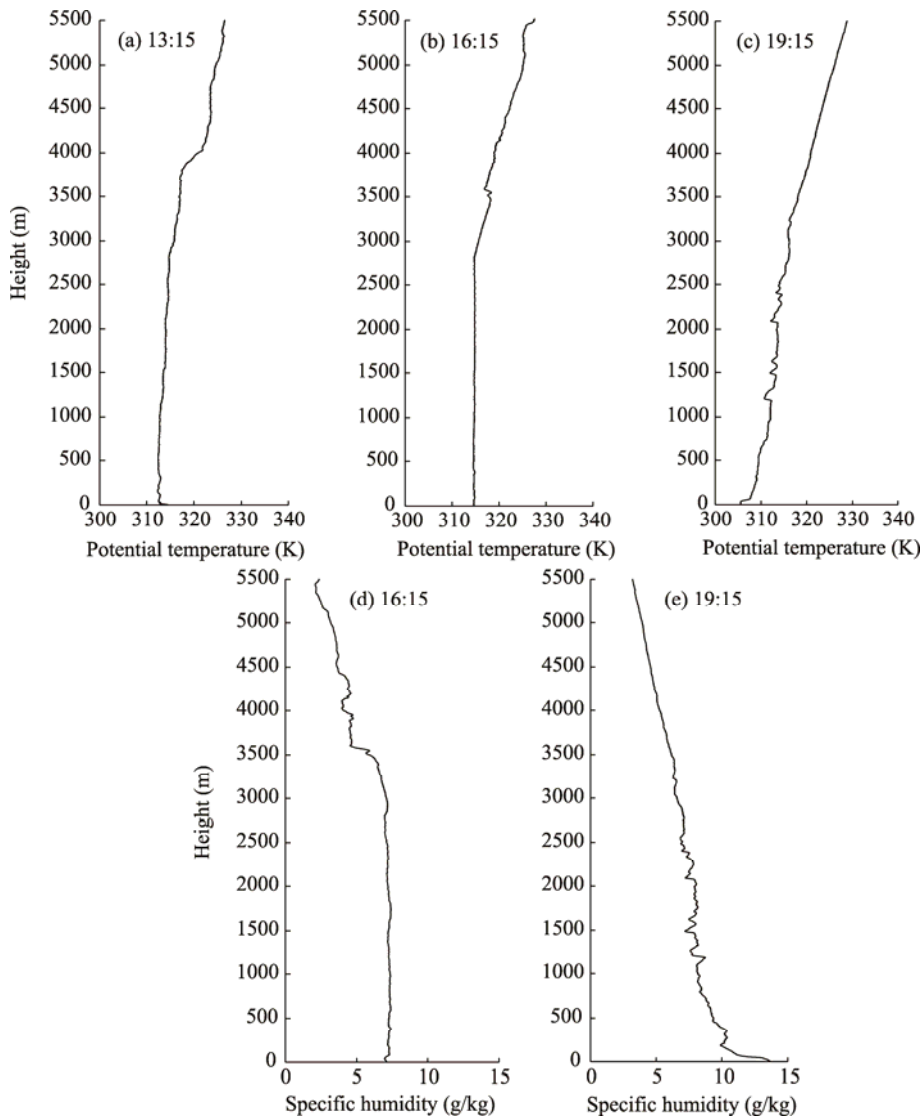


Fig. 8 Atmospheric potential temperature and specific humidity profiles at different atmospheric heights in the hinterland of Taklimakan Desert at different observation times on 1 July 2015

The boundary layer structure at 13:15 was clearly observed and the vertical variation of

potential temperature below 2,900 m changed slightly, basically maintaining a relatively uniform and constant state (Fig. 8). This means that the height of convective boundary layer was about 2,900 m. At 16:15, the profiles of potential temperature and specific humidity both illustrated that the convective boundary layer was about 2,900-m thick. From 16:30 to 18:30, a short-time precipitation occurred. After the rain, the potential temperature increased with increasing height from the ground surface, but the specific humidity decreased with increasing height. The structure of convective boundary layer was destructed remarkably, making the vertical structure of atmospheric boundary layer was difficult to be distinguished.

The above analysis showed that precipitation process is a cooling and moistening process, and also an energy release process. Strong convective precipitation can alter the heat to the atmosphere in a very short time, destroy the atmospheric boundary layer structure significantly and reduce the thickness of atmospheric boundary layer.

4 Discussion

Recognizing the characteristic of atmospheric boundary layer over Taklimakan Desert is conducive to improve the model parameters and the accuracy and precision of weather and climate simulations. In this study, we used the GPS sounding system to detect the desert atmospheric boundary layer, and the analysis showed that the summer atmospheric boundary layer is very thick and can develop to 4,000-m height. Xu et al. (2014) studied the atmospheric boundary layer structure of this region by the NCEP reanalysis data, and pointed out that the thickness of convective boundary layer can reach 3,000–4,000 m. Our study verified the phenomenon that the atmospheric boundary layer with supernormal thickness exists over Taklimakan Desert in summer, which could provide a reference and scientific bases for the regional numerical models to better represent the atmospheric boundary layer.

Wei et al. (2005), Zhang and Wang (2008) and Li et al. (2014) have conducted observational studies on atmospheric boundary layers over Jinta oasis, Dunhuang region and Badain Jaran Desert in the arid areas of Northwest China, respectively. They found that on clear days in summer, the maximum height of convective boundary layer in Dunhuang may exceed 4,000 m, the height of convective boundary layer in Jinta oasis of Hexi Corridor is about 3,500 m and the height of convective mixing layer over Badain Jaran Desert can reach up to 3,000 m. Compared with these findings, the height of convective boundary layer in summer in Taklimakan Desert is much closer to that in Dunhuang, and a bit higher than those in Badain Jaran Desert and Jinta oasis. On 25 June 2015, it was a hot and cloudy day in the study area. The reason why the convective boundary layer on this day could develop to 4,000-m height is that, in addition to the heating effect of ground surface to the atmosphere, the thick residual layer over nighttime is a brief contributor. This finding is agreed with the result of Zhang et al. (2007) for Dunhuang, Gansu province.

In addition, sand-dust weather often occurs in Taklimakan Desert in spring and summer, which can affect the development of atmospheric boundary layer remarkably. Under such weather condition, the height of atmospheric boundary layer descends, and its maximum thickness is about 900 m. This phenomenon can illustrate why the height variability of atmospheric boundary layer is very large in Taklimakan Desert to some extent. Thus, when conducting the parameterization of boundary layer in Taklimakan Desert, we should sufficiently take into account the weather phenomena and its occurrence frequency to ensure the accurate description to the height of boundary layer.

Since there were several different weather processes during our study period, we failed to obtain the densely-observed sounding data on very hot and clear days, we also did not observe the convective boundary layer with deep thickness (reaching 5,500 m) as observed in the Sahara Desert (Gamo, 1996; Cuesta et al., 2008; Marsham et al., 2008; Messenger et al., 2010). Of course, we believe that the convective boundary layer in Taklimakan Desert would develop more thickly along with the extremely high temperature, but this needs more radiosonde observations. By the means of numerical simulation, we can study more deeply the unique convective boundary layer process and its developing mechanism in the future.

5 Conclusions

Using the GPS sounding system, we carried out the detection for the summer atmospheric boundary layer in the hinterland of Taklimakan Desert, analyzed the vertical structures of daytime convective boundary layer and nighttime stable boundary layer, and discussed the impacts of sand-dust and precipitation processes on desert atmospheric boundary layer structures. The main conclusions are as follows.

(1) In summer, the nighttime stable boundary layer in the hinterland of Taklimakan Desert is 400–800-m thick, and the residual mixing layer above it still clearly reserves the top covers of daytime mixing layer and inversion layer. The thickness of the daytime convective boundary layer is very large and the height can reach up to 4,000 m. The atmospheric residual layer with deep thickness at nighttime provides very favorable thermodynamic background for the development of convective boundary layer during the daytime. This finding verifies further the phenomenon that the atmospheric boundary layer with extreme thickness exists over Taklimakan Desert in summer.

(2) Sand-dust event destroyed the structures of nighttime stable boundary layer and daytime convective boundary layer to some extent. The dust particle swarm can weaken the solar radiation absorbed by the ground surface, impact the heat to the atmosphere and then restrain the development of daytime convective boundary layer. On 26 June 2015, i.e. the sand-dust day, the maximum height of convective boundary layer was about 900 m, which was far lower than that on 25 June 2015.

(3) Severe convective precipitation can change the heating of the atmosphere in a very short time. At the same time, it can also destroy the desert atmospheric boundary layer structure. The height of boundary layer becomes very low due to precipitation.

Acknowledgements

This work was supported by the National Natural Science Foundation of China (41575008, 41305035) and the Project for Public Good Dedicated to the Meteorological Sector in China (GYHY201406001).

References

- Angevine W M, White A B, Avery S K. 1994. Boundary-layer depth and entrainment zone characterization with a boundary-layer profiler. *Boundary-Layer Meteorology*, 68(4): 375–385.
- Charney J G. 1975. Dynamics of deserts and drought in the Sahel. *Quarterly Journal of the Royal Meteorological Society*, 101(428): 193–202.
- Cuesta J, Edouart D, Mimouni M, et al. 2008. Multiplatform observations of the seasonal evolution of the Saharan atmospheric boundary layer in Tamanrasset, Algeria, in the framework of the African Monsoon Multidisciplinary Analysis field campaign conducted in 2006. *Journal of Geophysical Research: Atmospheres*, 113(D23): D00C07.
- Cunnington W M, Rowntree P R. 1986. Simulations of the Saharan atmosphere-dependence on moisture and albedo. *Quarterly Journal of the Royal Meteorological Society*, 112(474): 971–999.
- Dearldorff J W. 1970. Convective velocity and temperature scale for the unstable planetary boundary layer and for Rayleigh convection. *Journal of the Atmospheric Sciences*, 27(8): 1211–1213.
- Gamo M. 1996. Thickness of the dry convection and large-scale subsidence above deserts. *Boundary-Layer Meteorology*, 79(3): 265–278.
- Garratt J R. 1992. *The Atmospheric Boundary Layer*. Cambridge: Cambridge University Press, 1–3.
- Garratt J R. 1993. Sensitivity of climate simulations to land-surface and atmospheric boundary-layer treatments-a review. *Journal of Climate*, 6(3): 419–448.
- Gornitz V, Nasa. 1985. A survey of anthropogenic vegetation changes in West Africa during the last century-climatic implications. *Climatic Change*, 7(3): 285–325.
- He Q. 2009. Observation study of atmospheric boundary layer structure and land atmosphere interaction in the Tazhong of Taklimakan Desert. PhD Dissertation. Nanjing: Nanjing University of Information Science & Technology, 80–100. (in Chinese)
- He Q, Jing L L, Yang X H, et al. 2010a. Analysis on O₃ concentration and affecting factors for boundary-layer in hinterland of

- Taklimakan Desert in Autumn. *Plateau Meteorology*, 29(1): 214–221. (in Chinese)
- He Q, Liu Q, Yang X H, et al. 2010b. Profiles of atmosphere boundary layer Ozone in winter over hinterland of Taklimakan Desert. *Journal of Desert Research*, 30(4): 909–916. (in Chinese)
- Henderson-Sellers A. 1980. Albedo changes-surface surveillance from satellites. *Climatic Change*, 2(3): 275–281.
- Hu Y Q, Gao Y X. 1994. Some new understandings of processes at the land surface in arid area from the HEIFE. *Acta Meteorologica Sinica*, 52(3): 285–296. (in Chinese)
- Huang Q, Marsham J H, Parker D J, et al. 2010. Simulations of the effects of surface heat flux anomalies on stratification, convective growth, and vertical transport within the Saharan boundary layer. *Journal of Geophysical Research: Atmospheres*, 115(D5), doi: 10.1029/2009JD012689.
- Hyun Y K, Kim K E, Ha K J. 2005. A comparison of methods to estimate the height of stable boundary layer over a temperate grassland. *Agricultural and Forest Meteorology*, 132(1–2): 132–142.
- Lare A R, Nicholson S E. 1990. A climatonic description of the surface energy balance in the central Sahel. Part I: shortwave radiation. *Journal of Applied Meteorology*, 29(2): 123–137.
- Li J G, Ao Y H, Li Z G, et al. 2014. Characteristics of atmospheric boundary layer over the Badain Jaran desert in summer. *Journal of Desert Research*, 34(2): 488–497. (in Chinese)
- Liu Y Q, He Q, Zhang H S, et al. 2012. Improving the CoLM in Taklimakan Desert hinterland with accurate key parameters and an appropriate parameterization scheme. *Advances in Atmospheric Sciences*, 29(2): 381–390.
- Marsham J H, Parker D J, Grams C M, et al. 2008. Observations of mesoscale and boundary-layer scale circulations affecting dust transport and uplift over the Sahara. *Atmospheric Chemistry and Physics*, 8(23): 6979–6993.
- Messenger C, Parker D J, Reitebuch O, et al. 2010. Structure and dynamics of the Saharan atmospheric boundary layer during the West African monsoon onset: observations and analyses from the research flights of 14 and 17 July 2006. *Quarterly Journal of the Royal Meteorological Society*, 136(S1): 107–124.
- Qiao J. 2009. The temporal and spatial characteristics of atmospheric boundary layer and its formation mechanism over arid region of northwest China. MSc Thesis. Beijing: Chinese Academy of Meteorological Sciences, 6–12. (in Chinese)
- Redelsperger J L, Guichard F, Mondon S. 2000. A parameterization of mesoscale enhancement of surface fluxes for large-scale models. *Journal of Climate*, 13(2): 402–421.
- Seibert P, Beyrich F, Gryning S E, et al. 2000. Review and intercomparison of operational methods for the determination of the mixing height. *Atmospheric Environment*, 34(7): 1001–1027.
- Sivakumar M V K. 2007. Interactions between climate and desertification. *Agricultural and Forest Meteorology*, 142(2–4): 143–155.
- Stull R B. 1988. *An Introduction to Boundary Layer Meteorology*. Dordrecht: Kluwer Academic Publisher, 649.
- Su C X, Hu Y Q. 1987. The structure of the oasis cold island in the planetary boundary layer. *Acta Meteorologica Sinica*, 45(3): 322–328. (in Chinese)
- Takemi T. 1999. Structure and evolution of a severe squall line over the arid region in northwest China. *Monthly Weather Review*, 127(6): 1301–1309.
- Wang M Z, Wei W S, He Q, et al. 2012. Radar wind profiler observations of convective boundary layer during clear-air days over Taklimakan desert. *Meteorological Monthly*, 38(5): 577–584. (in Chinese)
- Wei Z G, Lü S H, Hu Z Y, et al. 2005. A primary research on the characteristics of wind, temperature and humidity in the boundary layer over Jinta summer. *Plateau Meteorology*, 24(6): 846–856. (in Chinese)
- Wen Y T, Miao Q L, He Q, et al. 2010. Observations on turbulence intensity and turbulent kinetic energy of surface layer in spring and summer in Taklimakan hinterland. *Journal of Desert Research*, 30(2): 439–444. (in Chinese)
- Xu X D, Wang Y J, Wei W S, et al. 2014. Summertime precipitation process and atmospheric water cycle over Tarim Basin under the specific large terrain background. *Desert and Oasis Meteorology*, 8(2): 1–11. (in Chinese)
- Zhang Q. 2007. Study on depth of atmospheric thermal boundary layer in extreme arid desert regions. *Journal of Desert Research*, 27(4): 614–620. (in Chinese)
- Zhang Q, Zhao Y D, Wang S, et al. 2007. A study on atmospheric thermal boundary layer structure in extremely arid desert and gobi region on the clear day in summer. *Advances in Earth Science*, 22(11): 1150–1159. (in Chinese)
- Zhang Q, Wang S. 2008. A study on atmospheric boundary layer structure on a clear day in the arid region in northwest China. *Acta Meteorologica Sinica*, 66(4): 599–608. (in Chinese)
- Zhang Q, Zhang J, Qiao J, et al. 2011. Relationship of atmospheric boundary layer depth with thermodynamic processes at the land surface in arid regions of China. *Science China Earth Sciences*, 54(10): 1586–1594.